

Surface Characteristics, Properties and Wear Resistance OF TiB₂ BASED Hard-Alloy Coatings Obtained by Electrospark Deposition at Negative Polarity on Ti6Al4V Alloy

Todor Penyashki^{a,*}, Georgi Kostadinov^a, Mara Kandeveva^b, Antonio Nikolov^b, Rayna Dimitrova^b, Valentin Kamburov^b


^aInstitute of Soil Science, Agrotechnologies and Plant Protection „N. Pushkarov“, Agricultural Academy, Sofia, Bulgaria,

^bTechnical University of Sofia, Bulgaria.

Keywords:

Electrospark deposition
Coatings
Surface roughness
Microhardness
Wear resistance

* Corresponding author:

Todor Penyashki 
E-mail: tpenyashki@abv.bg

Received: 30 June 2023

Revised: 24 July 2023

Accepted: 15 August 2023

ABSTRACT

In the present work, the possibilities of improving the surface properties of titanium alloy Ti6Al4V by electrospark deposition (ESD) at negative polarity were investigated. The coatings were deposited with a TiB₂-TiAl-based hard-alloy electrode with nano-sized additives of NbC and ZrO₂. The effect of polarity in ESD at low pulse energy (0.01-0.07 J) on the surface roughness, thickness, composition and structure of coatings was studied by profilometric, metallographic, XRD, SEM and EDS methods. In both polarities, dense and uniform coatings were obtained with roughness and thickness, which could be varied by changing the ESD modes within the range Ra=1.5÷4.5 μm, δ= 6÷20 μm and microhardness from 9 to 12 GPa, respectively. It was found that the negative polarity coatings obtained are denser and uniform with higher thickness, lower roughness, finer structure, and lower coefficient of friction, and can be successfully used to reduce the surface roughness and defects of 3D printed titanium alloy. Abrasion and erosion wear tests showed that the wear resistance of coated titanium surfaces at both polarities was 2.2 to 3.5 times higher than that of the substrate. Coatings deposited in positive polarity demonstrated higher resistance to abrasive wear, while those in negative polarity are more resistant to erosive wear.

© 2023 Published by Faculty of Engineering

1. INTRODUCTION

At present, to improve the low surface hardness and low wear resistance of titanium and its alloys [1-3], various surface modification methods such as ion nitriding, laser and electron beam treatments,

physical and chemical vapor phase deposition (PVD) and (CVD), gas flame and plasma spraying, etc. are used [4-8]. These methods are not always applicable due to various limitations such as high cost and process complexity, complex and expensive equipment, environmental pollution,

unfavorable structural and thermal deformation of the substrate, low adhesion, etc. Most of the limitations mentioned above can be overcome by electrospark deposition /ESD/ [9-11]. Due to its simplicity and versatility, flexibility, cost-effectiveness, and low heat input, this method is found to be suitable for improving the hardness, wear resistance, and corrosion resistance of titanium surfaces [11,12,13-19]. The main advantages of this process include non-polluting, versatile, simple and affordable technology as well as easiness of deposition of metal coatings under normal weather conditions. A strong metallurgical bond of the coating to the titanium substrate is achieved with low thermal impact and absence of heating and deformation of the coated product, low material and energy costs. One or more consecutive passes of the electrode may perform deposition over the substrate surface. The result is the formation of a thin surface layer with a supercooled (modified) structure [12], with a new relief and different surface properties from the original ones, which are controlled by the electrical and physical parameters of the mode and composition of the electrode material [9,10,13-18]. This allows for obtaining fundamentally new materials and structures, including nanostructural effects, which cannot be obtained under conventional metallurgical conditions [9-12,15,17-21].

A specific phenomenon in ESD of titanium surfaces is the initial erosion of titanium substrates and the formation of relatively deep craters on the coated surface [13,14], and as a result - the appearance of structural defects of coatings- relatively high roughness and the presence of irregularities and micropores in the surface layer. It is possible to reduce these defects in various ways - by using an inert environment, coating electrodes of graphite and certain metals and alloys, by additional laser and other treatments [13,14,15,18,20], but they complicate the technology and the deposition process, increasing the time and cost of deposition. The easiest way to reduce the surface defects is to reduce the single pulse energy (current, capacitance and pulse duration) [15-18]. This results in fewer surface defects and lower roughness, but also lower thickness and less amount of wear-resistant phases and compounds in the coating composition. The use of lower energy with an extremely short duration of electrical pulses - 10^{-6} - 10^{-5} s, however, creates conditions for the formation of a higher amount

of amorphous and nanostructured phases in the composition of coatings, which, according to many authors [17-21], favorably affects their wear and corrosion resistance.

Combining higher electrode material transfer on titanium surfaces, reduction of titanium substrate erosion, and good coating density, uniformity and low roughness are conflicting objectives that cannot be achieved by ESD process mode parameters only.

One of the important parameters of the electrodeposition process is the polarity of the electrodes. In ESD, positive polarity (+) is used (the electrode is the anode), and usually, the predominant transport direction of erosion products is from the anode to the cathode. However, the analysis of the surface layers of the electrodes at the ESD shows traces of erosion at both the anode and the cathode. Studies devoted to volumetric EDM have shown that the reverse/negative polarity (-) when the electrode is the cathode, at low current and low pulse duration provides cleaner and smoother surfaces with lower roughness than that at straight/positive polarity and with increased wear of the processing electrode [22-25]. The analysis of the literature and experimental data shows that despite the differences in spark-plasma discharge behavior in liquid and air environments, at low pulse energy and electrode negative polarity in ESD it is possible to obtain a dense coating with improved uniformity, reduced roughness, initial erosion of titanium substrates and reduced surface defects.

In this regard, the aim of the present work is to perform a comparative study of the properties of ESD-produced coatings on titanium surfaces at positive and negative polarity with low pulse energy and to evaluate the possibilities of improving the tribological characteristics of titanium surfaces by ESD with negative (-) polarity.

2. MATERIALS AND METHODS

The study is based on the hypothesis that the change of polarity results in a simultaneous increase in material removed and a decrease in the size of the erosion craters on the surface of the substrate, i.e. a smoother and uniform layered surface is obtained.

2.1 ESD equipment, substrates, electrodes

ESD equipment: To obtain less structural defects coatings with low roughness, ESD equipment with a low pulse energy of 0.01-0.07 J was used - an apparatus with a vibrating electrode - "Carbide Hardedge" (England, USA). The mode parameters are presented in Table 1. The coatings are applied with positive (+) and negative (-) electrode polarity.

Table 1. Regimes for ESD with vibrating electrode.

Nº of regimes	1	2	3	4	5	6
Capacity, μF	1.5	3.5	5	7	10	20
Pulse energy $E \cdot 10^{-2}, \text{J}$	0.5	1	1.6	2	3	7

Substrates: Model plates of popular titanium alloy Ti-6Al-4V and technical titanium – Ti-GR2 (AISI UNS R R56200 and R50400) with square and rectangular shapes were used. The 5 mm thick, plates were produced in two ways:

- Cutting from round and square rods by EDM;
- Manufacturing by 3D printing and selective laser melting SLM.

Electrodes: Electrodes of $\text{TiB}_2\text{-TiAl}$, (74%Ti + 12%B + 14%Al) dispersive reinforced with 7% nano-sized ZrO_2 and NbC particle additives were used to form coatings with amorphous and nanostructured phases and to increase the microhardness and wear resistance of coated surfaces [18-21,25-30].

2.2 Methodology of measurements, research equipment

The roughness of the coatings was measured using TESA Rugosurf 10-10 G and AR-132B profilometers according to EN ISO 13565-2:1996, DIN 4776 (for parameter R_k), and the thickness δ of the coatings was determined with an indicator clock with an accuracy of 0.001 mm. Double-sided roughness measurement of the samples was performed in three sections in two perpendicular directions for each of the sections.

A Zwick 4350 hardness tester at a load of 2N was used to investigate the microstructure and microhardness (HV) of coatings according to ISO 6507-1.

Phase identification, microstructural analysis, analysis of topography, morphology and composition of the coatings were carried out using a Bruker D8 Advance X-ray diffractometer in "Cu K α " radiation and a scanning electron microscope (SEM-EDS) "EVO MA 10 Carl Zeiss" with built-in X-ray microanalyzer EDX system "Bruker".

The "CSM REVETEST Scratch Macrotester" was used to compare and digitally record the coefficient of friction (μ) and tangential force (F_t) of coatings under increasing normal load from 0 to 50 N at a rate of 10 N/mm.

Abrasive wear of the coated surfaces was investigated by comparative tests with a "thumb-on-disc" type tribotester in dry friction with fixed abrasive particles in planar contact under the following conditions: normal load 5 N; nominal contact area $2,25 \times 10^{-6} \text{ m}^2$; nominal contact pressure $1,74 \text{ N/cm}^2$, disc rotation speed 60 rpm; sliding speed 0,239 m/s; abrasive surface - Corundum Nº 1200. Mass wear was defined as a difference between the initial mass of the specimen "m0" and its mass "mi" after a certain number of friction cycles: $m = m_0 - m_i$, mg. The mass of the samples before and after a particular friction path was measured with an electronic balance WPS 180/C/2 with an accuracy of 0.1 mg.

The wear intensity was defined as the amount of wear per unit friction work: $I = m / (P \cdot L)$, mg/Nm, where m is the solid wear over the test time, P-normal load, and L-travelled friction path. The wear resistance was defined as the reciprocal of the wear intensity.

The erosive wear of the coatings was tested by an air jet carrying abrasive particles in an atmospheric environment. The double-phase "air-abrasive particle" mixture interacts at a 90° angle with the coating surface [31,32].

There were determined: Mass flow rate of abrasive material; Mass erosion wear rate as a difference between the mass of the specimen before and after treatment with the double-phase jet; Mass wear rate as the mass of coating destroyed per unit time; Erosion intensity as a ratio of mass wear rate and mass flow rate of abrasive phase in the jet, Erosion resistance as a reciprocal value of wear intensity [32]. The test conditions are shown in Table 2.

Table 2. Parameters used in the erosive wear testing.

Test parameters	Value
Solid particles material	corundum Al ₂ O ₃
Maximum size of the particles	600 μm
Air stream pressure	0.1 MPa
Particles flow	140 g/min
Particles impact angle	90°
Distance between the sample and the nozzle	10 mm
Duration of the test	5 minutes
Ambient temperature	21° C

3. RESULTS AND DISCUSSION

3.1 Comparison of the topography, roughness, structure and microhardness of the coatings

Fig. 1 shows at different magnification the type of erosion craters obtained with positive polarity ESD on the titanium surface.

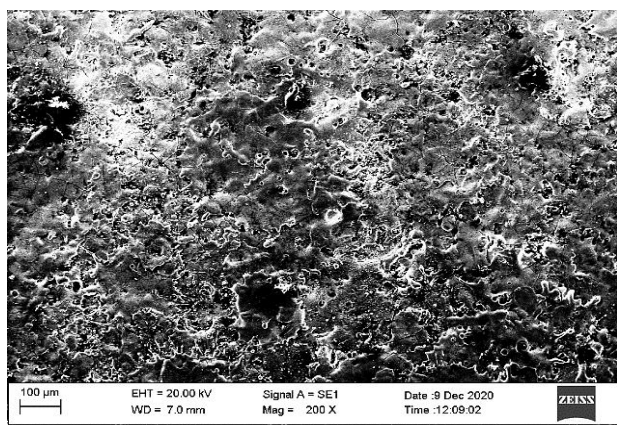
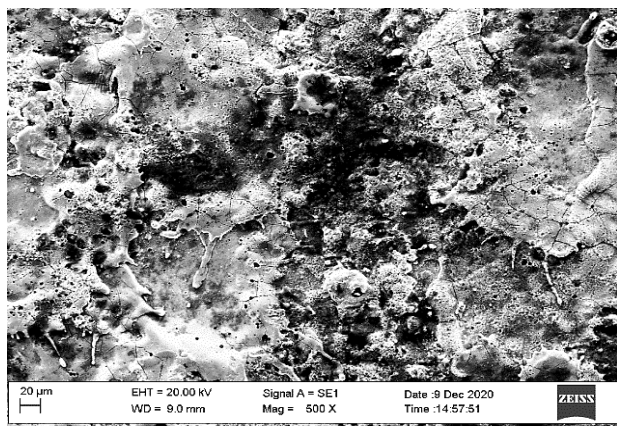
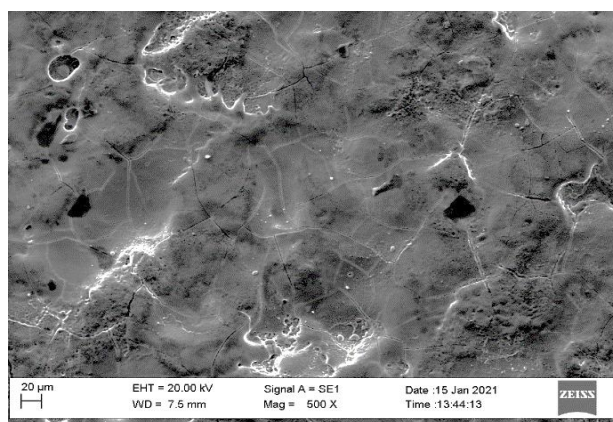


Fig. 1. Erosion craters at (+) polarity and pulse energy 0.07 J.

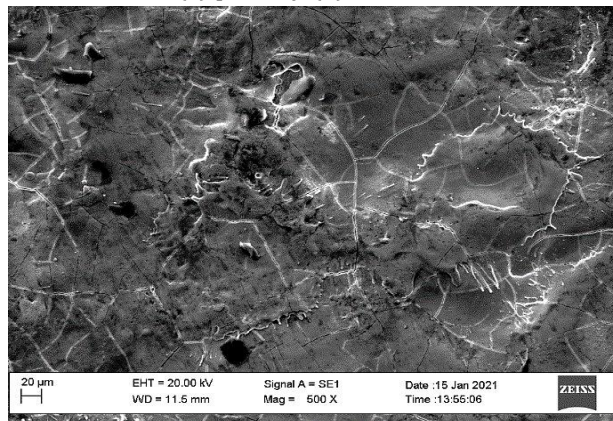
Figs. 2 and 3 show typical SEM images of the texture and relief of the coated surfaces at both polarities obtained at different pulse energy modes.

It can be seen that at both pulse energies, as well as positive and negative polarity, the surface of the coatings is relatively uniform and homogeneous. This is probably due to the presence of the nano-sized particles of the electrode material, as well as the good solubility of the electrode material components in the titanium substrate, and also the presence of TiAl, which has a lower melting temperature and "spreads" more uniformly on the titanium surface. Individual craters from the erosion of titanium cathodes, protrusions of accumulated anode material, smooth glass-like areas in between are clearly distinguishable.

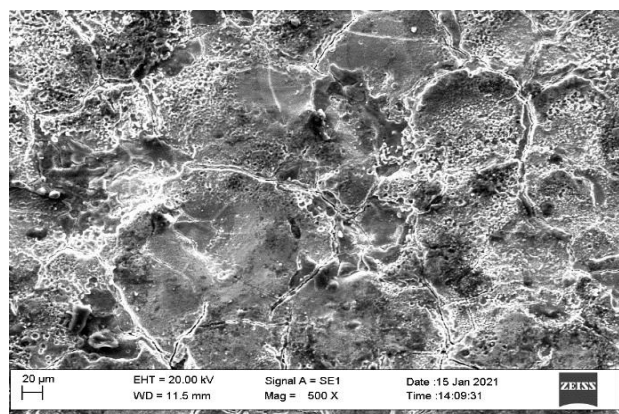
It can be seen from Figs. 2 and 3 that the coatings are mainly formed by melt, which is more evident at the (-) polarity. The sections with amorphous structure as well as the products of brittle fracture of the electrode are distinguishable.



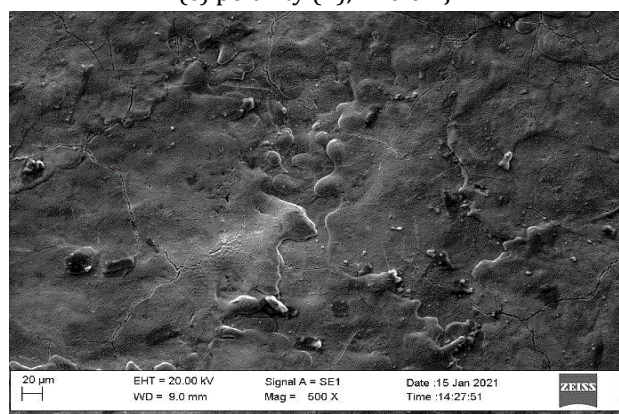
(a) polarity (+), E=0.03 J



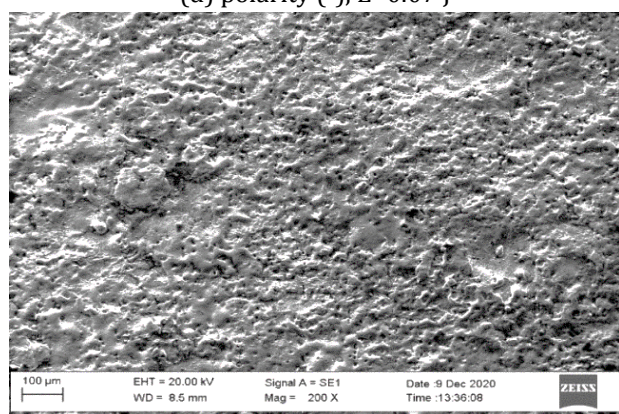
(b) polarity (-), E=0.03 J



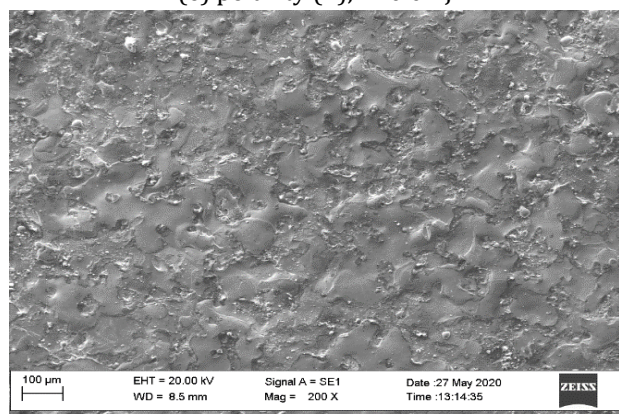
(c) polarity (+), E=0.07 J



(d) polarity (-), E=0.07 J



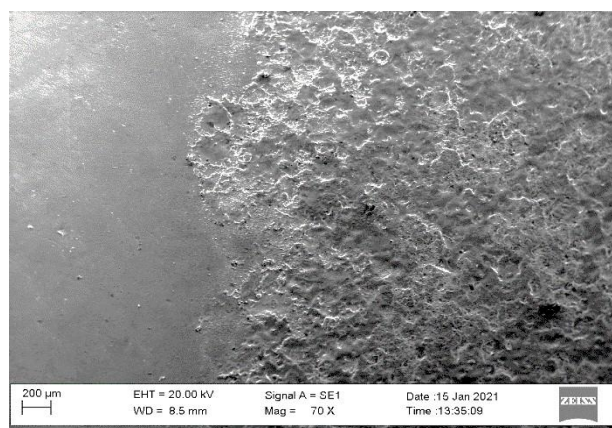
(e) polarity (+), E=0.07 J



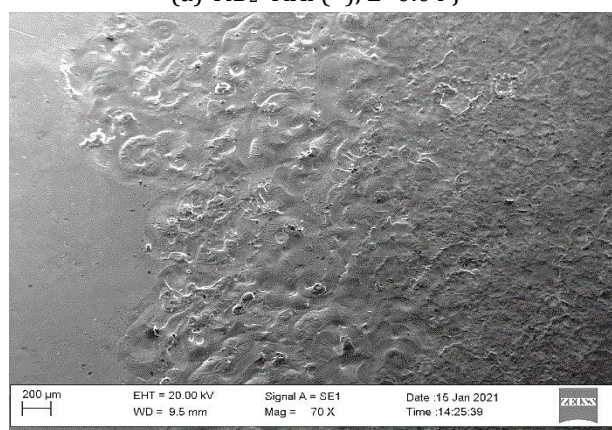
(f) polarity (-), E=0.07 J

Fig. 2. SEM images of topography of coatings on Ti6Al4V with (TiB₂-TiAl)_{nano} electrode.

The predominance of the spherical particle shape (Fig. 2b,d,f) indicates that the destruction of the processed material takes place in the molten state. At a pulse energy of 0.07 J, both larger and deeper erosion craters and traces of brittle electrode destruction - irregularly shaped protrusions - are observed. The last ones are more pronounced in coatings obtained with (+) polarity - (Fig.1 and Fig.2c).



(a) TiB₂-TiAl (+), E=0.04 J



(b) TiB₂-TiAl (-), E=0.04 J

Fig. 3. Topography (SEM) of the interfacial zone of ESD coatings on Ti6Al4V.

It can be seen that the coatings deposited at both polarities have a similar structure and relief, but differ in the amount of erosion craters, smooth areas and the height of micro-roughness. Comparison of the polar effect shows that the coatings obtained at (-) polarity are smoother and more uniform, have a more homogeneous structure with fewer and smaller sized protrusions and craters and smoother transitions between individual droplets.

At the positive polarity, the impinging pulse creates a microcavity surface and negative

shapes are formed on the substrate surface (Fig. 2a,c,e), also in the intermediate zone along the contact with the uncoated surface (Fig. 3a). There are also more protuberant and less spilt areas (Fig. 2a,c,e and Fig. 3a). As the pulse energy increases, the height of the micro irregularities also increases, and the amount of smooth glass-like areas decreases. The height of single clusters and protrusions also increases.

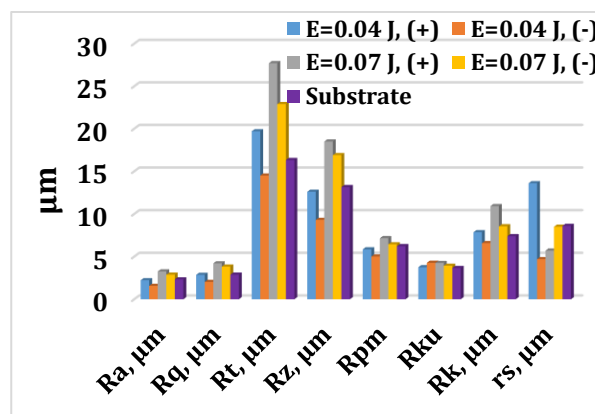
Table 3 shows the averaged values of substrate growth, thickness and microhardness obtained at (+) and (-) polarity at different pulse energy. The values of the height and functional roughness parameters of the coatings are shown in Fig. 4 for different initial substrate roughness. Roughness parameter designations are according to EN ISO 13565-2:1996 standard.

Table 3. Substrate increment Δs , thickness δ , microhardness HV and coating roughness parameters.

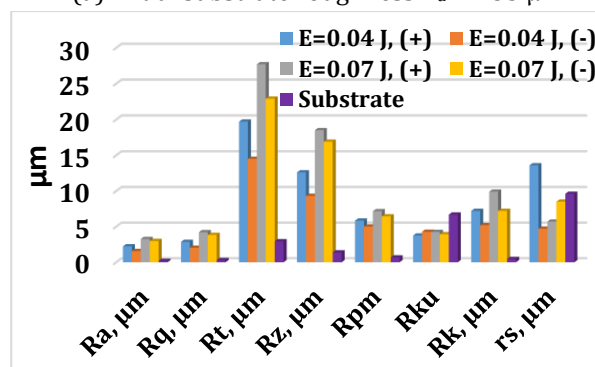
Parameters	E=0.04 J Polarity (+)	E=0.04 J Polarity (-)	Sub- strate
Δs , mg	3,3	2,7	-
δ , μm	24, 17	21, 30	-
HV min, GPa	8,96	9.71	3.41
HV max, GPa	14.88	15.67	4.07
HV avrg, GPa	11.32	12.85	3.71
Parameters	E=0.07 J Polarity (+)	E=0.07 J Polarity (-)	Sub- strate
Δs , mg	4,4	5,6	-
δ , μm	28,31	33	-
HV min, GPa	9.31	10.01	3.41
HV max, GPa	15.64	15.91	4.07
HV avrg, GPa	13.09	13.87	3.71

As can be seen, most of the parameters of the coatings obtained with (-) polarity are lower. It is found that at higher initial roughness of the uncoated titanium surfaces, the most commonly used in practice parameters R_a , R_q , R_z , R_{pm} , R_{ku} at the lower pulse energy mode and (-) polarity (Fig. 4a) have lower values than those of the substrate, while the values obtained at (+) polarity are comparable, or higher than those of the substrate. At the higher pulse energy of 0.07 J in both polarities, most of the coating roughness parameters take values higher than those of the substrate but close to those of Fig. 4a. It can also be observed (Fig. 2, 3 and Fig.4) that as the pulse energy increases, the roughness parameters of the coated surfaces increase.

Increasing the energy of the current spark creates a wider and deeper crater on the titanium surface, which also forms a higher roughness. The negative polarity resulting from the smaller size of the formed craters provides lower surface roughness. The obtained data are in accordance with the results presented by Khan, Gavali, Prakash et al [22-25] who analyzed the effect of low pulse energy in EDM processing and validate that the low pulse energy and negative polarity result in improved surface roughness.



(a) initial substrate roughness $R_a \approx 2.35 \mu\text{m}$



(b) initial substrate roughness $R_a \approx 0.19 \mu\text{m}$

Fig. 4. Coating roughness parameters obtained with different electrode polarity

In parallel with the roughness, the thickness and microhardness of the coatings increase, which takes values up to three times higher than that of the substrate (Table 3) [33]. The comparison of substrate growth, thickness and microhardness of the coatings obtained at both polarities shows that at (-) polarity the thickness of the coatings at $E = 0.04 \text{ J}$ is lower and at $E = 0.07 \text{ J}$ is higher than that at positive polarity. The microhardness of the negative polarity is up to 1 GPa higher than that of the positive polarity. Due to the presence of a matrix with lower hardness and a hard carbide phase, the individual measured microhardness values of the surface layer vary widely - Table 3.

3.2 X-ray phase analysis

Fig. 5 shows the X-ray phase diagrams of coatings obtained at both polarities. Comparison of the X-ray data at (+) and (-) polarity shows (Fig. 5, Table 4) that there is no significant difference between the spectral lines and the characteristic peaks obtained in (+) and (-) polarity mode, only the intensity and width of some of the X-ray peaks are different.

The main detected phases from electrode and substrate are Ti, TiB, TiB₂. AlTi. New phases

synthesized in the spark-plasma discharge process are also observed, the main ones are TiN, TiN_{0.3}, Al₃Ti, Ti₂O, and also traces of Al₂O₃ and AlN in small amounts. Noticeable is the presence of the triple compound (Ti₄N₃B₂)_{0.8}, the amount of which at E = 0.04 J in coatings applied with (-) polarity reaches ≈ 20%, and at (+) polarity - up to ≈ 30%. According to the literature data [34,35], this compound is referred to dispersion-hardened composite materials (DHCM) with high hardness and shows higher wear resistance than titanium nitrides and borides.

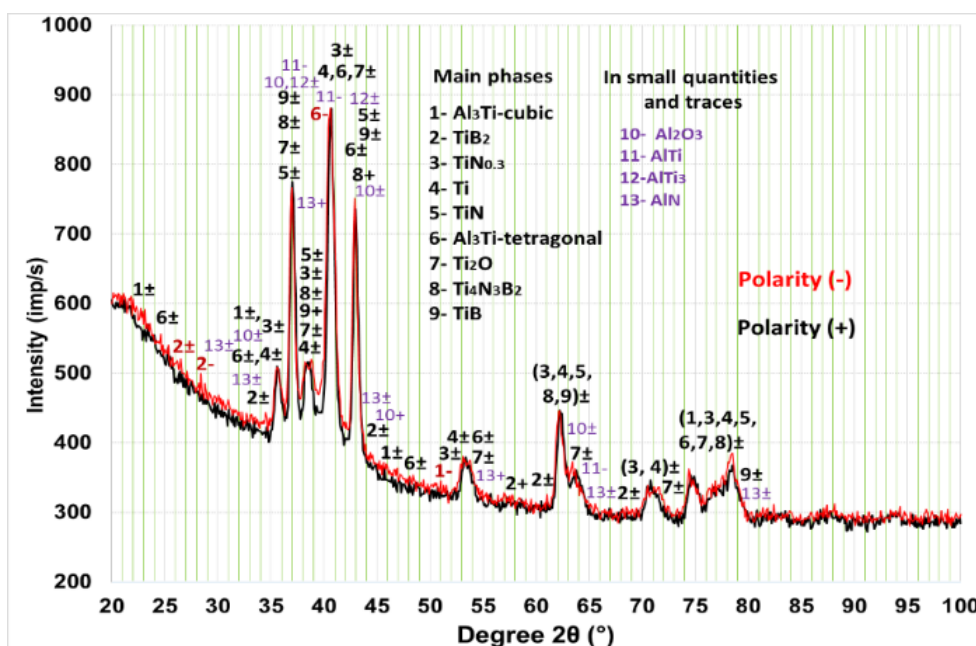


Fig. 5. X-ray diagram of coatings at (+) and (-) polarity and pulse energy E=0.04 J.

At the positive polarity, the amount of high-hardness and newly formed compounds TiB, TiAl₃, TiN_{0.3}, (Ti₄N₃B₂)_{0.8}, AlN is higher, while the amount of TiB₂, TiN, Al₂O₃, Ti₂O, AlTi is comparable or lower than that obtained at the (-) polarity. Differences in the composition of the coatings are found to be mainly quantitative. The other important new phase, TiN, has been detected in smaller amounts (6÷12%), but under certain conditions at (-) polarity the amount of TiN formed in the layer can increase up to 17 %. According to [36], higher wear resistance can be expected from combining TiN with TiB₂ than that of the two components separately. The formation of Al₂O₃, TiAl₃ and Ti₃Al in the layer according to [37] results in higher melting temperature, high elastic modulus, heat and oxidation resistance, also increased adhesion, hardness and wear resistance.

Table 4. Contents of the X-ray diagrams in positive (+) and negative (-) polarity.

Pulse energy E=0.04 J	polarity (-)	polarity (+)
Background radiation	92.84%	92.65%
Diffraction peaks	7.16%	7.35%
Peak area belonging to selected phases	5.70%	5.73%

The widening of the characteristic peaks of angle 2θ=35-40, 60-66, 70-82° is not only due to the formation of new compounds and solid solutions but also due to the structure refinement reaching an amorphous structure in individual sections. The presence of amorphous glass in electrospark coatings is reported in [12,15,19,21,29,30,35,36]. However, the presence of individual peaks in the X-ray diagrams also indicates the presence of crystals, which allows us to conclude that the coatings obtained with this electrode at both polarities have a mixed amorphous-crystalline structure.

The results of the X-ray phase analysis and SEM analysis make it possible to find that the change of electrode polarity and process parameters and pulse energy allows for to reduce the surface roughness, control of the composition, structure and geometrical characteristics of the coatings and obtain surfaces with desired composition, structure and properties.

3.3 Study of tribological characteristics of coatings

Fig. 6 shows the variation of the coefficient of friction and the friction force for coatings applied at (+) and (-) polarity as a function of the normal load. Compared with the untreated samples, the development of the coefficient of friction in the ESD samples shows irregular significant fluctuations at the beginning of the tests under normal loading up to ≈ 15 N. During the following period, as the normal load increased to 50 N, the coefficient of friction became stable and is kept relatively constant. For the coatings with both polarities, the coefficient of friction is in the range 0.4-0.55 - about 12-16% lower than that of the uncoated samples and almost does not change.

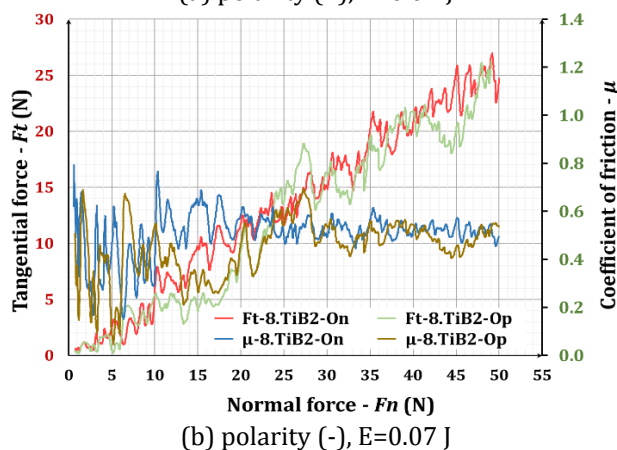
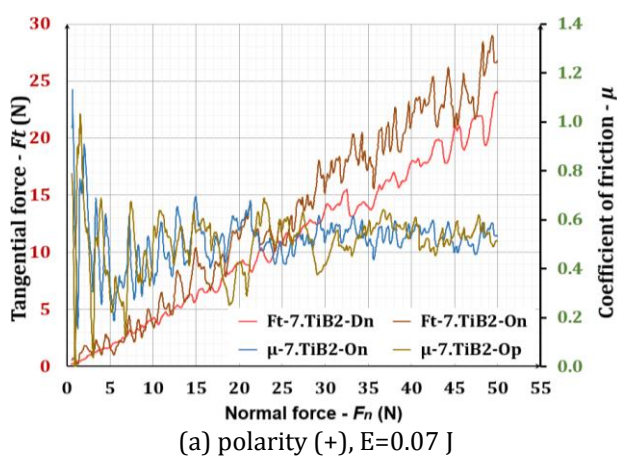


Fig. 6. Friction coefficient and friction force versus normal load for coatings applied with pulse energy E = 0.07 J.

At the higher pulse energy, the coefficient of friction is about 15% higher than that at energy 0.04 J, and its values at (-) polarity are 10-15% lower than those at (+) polarity, which is apparently the result of the better uniformity and lower roughness of the obtained at (-) polarity surfaces. The obtained coefficient and friction force values are close to those reported in the works [15,30].

Fig. 7 shows the mass wear development as a function of the friction path for coatings deposited at both polarities at two different pulse energy values, and Fig. 8 shows the wear and wear resistance of the coatings in the erosion tests.

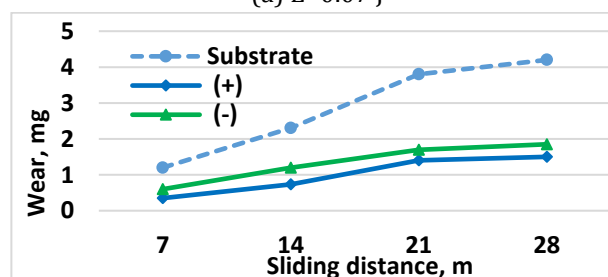
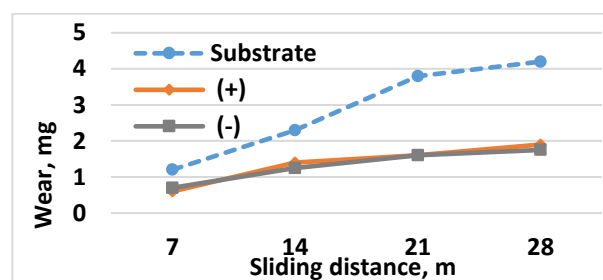


Fig. 7. Mass friction wear of coatings when deposited with (+) and (-) polarity on substrate - Ti6Al4V with TiB₂-TiAl_{nano} electrode at different energy

From the comparative friction test results - Fig. 7, it is found that the coated specimens at both polarities have 1.9 - 2.5 times lower wear than the uncoated ones. It is reasonable to suppose that the lower roughness and better uniformity of the deposited in (-) polarity coatings will also result in their lower wear, but due to the higher amount of solid phases in the (+) polarity, the wear values of the obtained in both polarities surfaces are similar. The wear at both energies is also similar, as those obtained at a pulse energy of 0.04 J show only up to 15-17% lower wear. At this energy, the coatings are more uniform, with finer structure, lower roughness (Fig. 3, 4, Table 3) and lower coefficient of friction, which contributes to their lower wear, and the differences in roughness obtained at positive (+) and negative (-) polarity are lower (Fig. 4). At the high energy, the unfavorable

influence of the higher roughness is balanced by the higher thickness and microhardness values and the larger amount of solid and intermetallic phases and the wear values at both pulse energies are similar. Observations show that in both polarities the wear of the coated surfaces occurs in the classic two stages: initial and normal wear. During the first stage, the most intense wear is observed on the studied surfaces, with a lower wear intensity on the surfaces deposited at (-) polarity. The analysis of the wear traces on the coated surfaces (Figs 9, 10) shows that at the beginning the abrasive particles wedge themselves between the tops of adjacent protrusions in the coating surface. Sliding friction and shear force result in the broken-off particles remaining in the wear trace.

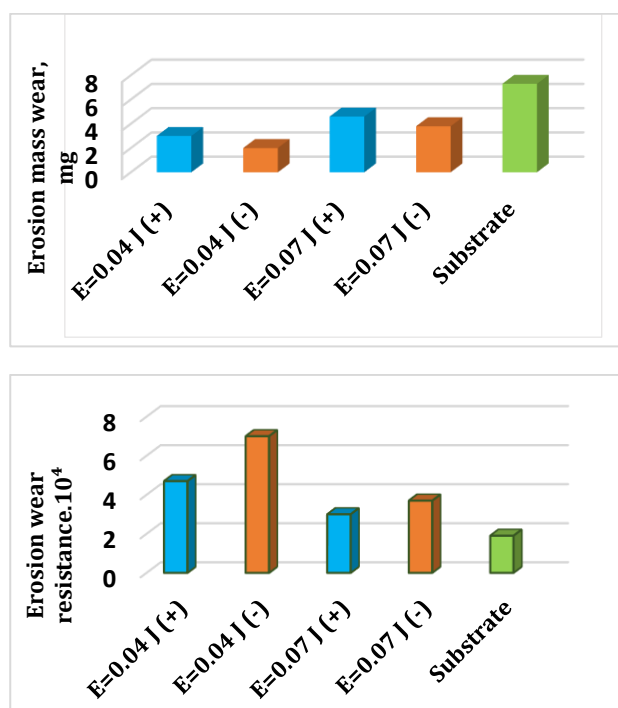


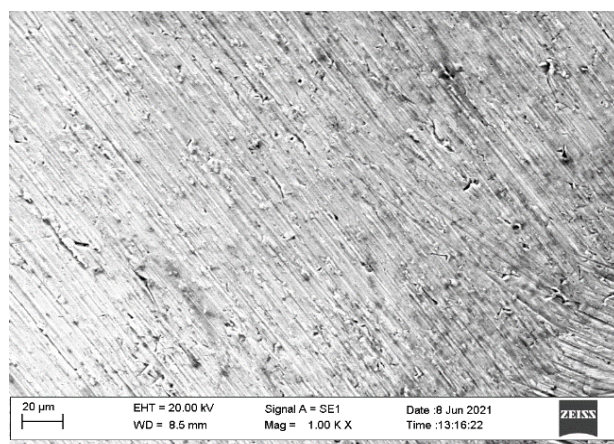
Fig. 8. Erosion wear and wear resistance of coatings deposited with (+) and (-) polarity on substrate - Ti6Al4V with TiB₂-TiAl_{nano} electrode at different energy.

Wear continues with the debonding of the coating material in the area of the protrusions, of the micropores and of the particles carried by brittle fracture of the electrode. The initiated cracks spread over the friction surface and then cause breaking off new coating particles. Plastic deformation and abrasive wear are dominant at the start of friction. The broken off hard particles are involved in the subsequent friction and contribute to increasing wear. The normal wear process has a monotonic character. The initial surface microgeometry changes over time and becomes smooth with fine shallow scratches, and craters,

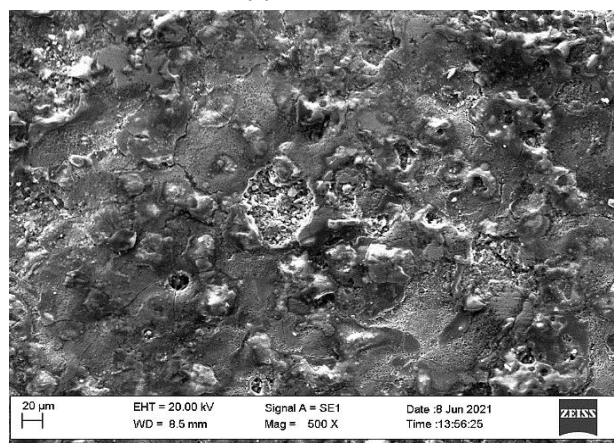
(Fig. 10). Wear is similar in coatings deposited with both polarities Fig. 10b, c. It is accompanied by microfractures and microcutting, and is concentrated towards the pores, microcracks and particles carried by brittle fracture of the electrode. However, ESD slows the development of wear over time. It is found from Fig. 7a and b that the ESD specimens reach a wear of ≈ 2 mg for a friction path of ≈ 30 m, and the uncoated titanium specimens reach this wear for a friction path of ≈ 10 m.

Wear of the substrate starts with scratching caused by the abrasive particles (Fig. 9a) and gradually progresses to predominantly abrasive adhesion, with craters forming on the surface. On the worn substrate surface numerous deep scratches, adhesion craters and cracks are observed, the size and quantity of which are much higher than those on the coated surfaces (Fig. 10a). The depth of penetration of the abrasive particles into the substrate is also greater than for coated surfaces.

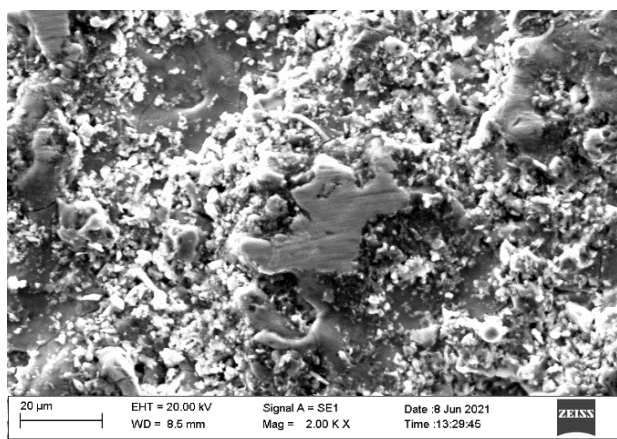
The erosion wear tests Fig. 8 show lesser wear on the surfaces coated at negative (-) polarity. The lowest wear has been found at pulse energy 0.04 J and negative (-) polarity.



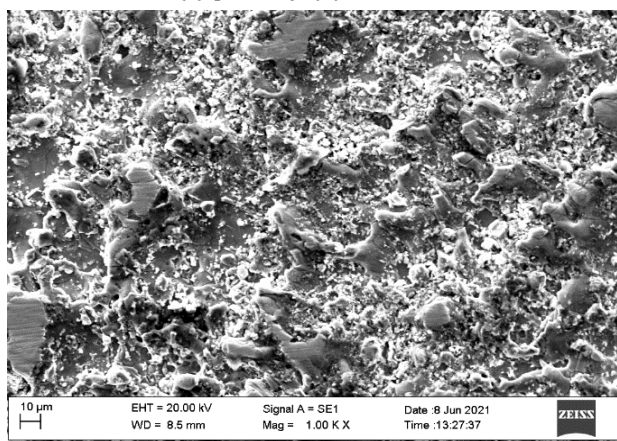
(a) Uncoated



(b) ESD detached protrusion from a brittle destruction



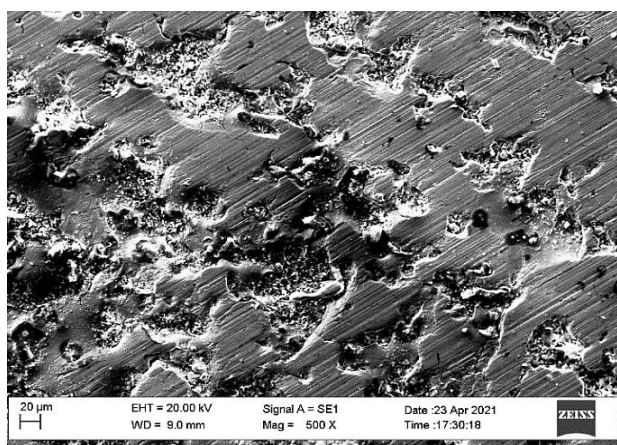
(c) polarity (+), E=0.07 J



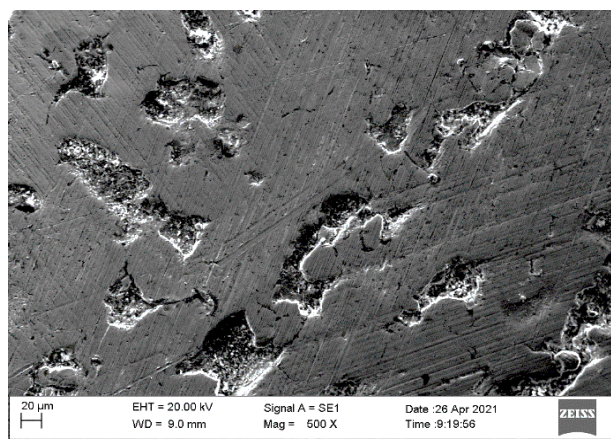
(d) polarity (-), E=0.07 J

Fig. 9. SEM images of surfaces at the beginning of wear - friction path 7 m.

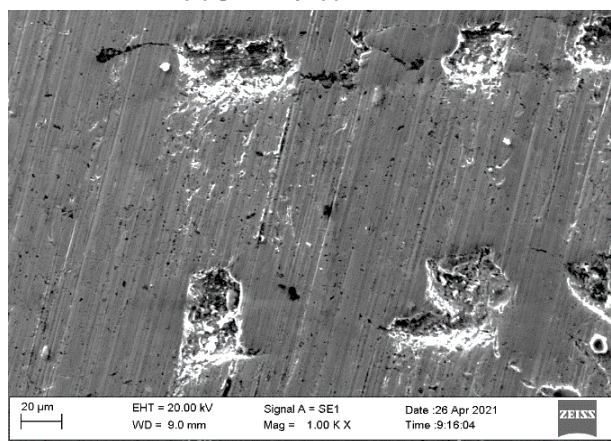
Obviously, in this type of tests, the lower roughness and smaller size and quantity of craters and protrusions on the titanium surface had a decisive influence on wear. At higher energies, the size and amount of particles from the brittle fracture of the electrode increases, which are not strongly bonded to the substrate and are more easily removed under the action of the air-abrasive jet.



(a) Uncoated



(b) polarity (-), E=0.04 J



(c) polarity (+), E=0.04 J

Fig. 10. SEM images of surfaces at a friction path of 28 m.

The data obtained and the description above are in good accordance with the results of studies by other researchers [38-40].

4. CONCLUSIONS

1. The polarity reversal in ESD with TiB₂-based hard-alloy electrodes with additions of nano components NbC, ZrO₂, stimulates the appearance of some processes favorable from the tribology point of view:

- reducing the depth and size of the initial craters on the titanium surface and, as a result, reducing surface roughness;
- formation of a surface with increased hardness on titanium alloys, which can play the role of a hard lubricating film and reduce the wear of friction surfaces;
- the formation of fine-grained structure as a result of material transfer in vapor and liquid phases as well as amorphous and

nano-structured phases due to the higher cooling rate resulting from the smaller size of the spark discharge, suggesting improved tribological characteristics;

- it has been found that the thickness of coatings obtained at (-) polarity is comparable and even slightly higher than that at positive polarity.

2. The hardness of negative polarity coatings increases by 10-15% over that of conventional positive polarity - apparently this is related to the formation of new compounds and amorphous phases in the modified titanium surfaces. The new compound synthesis and the increase in hardness occur together with a decrease in the size of the craters and of the individual structural components, and certain favorable changes in the structural-phase state of the coatings has been found.
3. At the higher pulse energy of 0.07 J, synthesis of secondary phases has been found for example (Ti₂N, TiN_{0.3}, AlN, Al₂O₃, Ti₂O), which is more clearly observed at negative (-) polarity, as well as increased content of new phases and titanium oxides. Obviously, these changes result in an improvement of the properties of the modified surfaces.
4. In the technique electrospark deposited coatings at negative (-) polarity can be used:
 - as a second (top) layer deposited on top of the first, thereby achieving two objectives: reducing the roughness of the coatings and achieving higher wear resistance;
 - as a first layer to obtain more uniform coatings with low roughness, and to reduce surface defects and roughness of 3D printed titanium surfaces.

Acknowledgement

The present work is based on researches that are funded from the Bulgarian National Science Fund of the Ministry of Education and Science under the project №KP-06-H37/19 "Technological features and regularities of creation of new high wear resistant composite coatings on titanium alloys by electrical spark deposition process".

This paper has been presented at the 18th International Conference on Tribology – SERBIANTRIB'23 17-19 May 2023, Kraguevac, Serbia.

REFERENCES

- [1] H. Dong, "Tribological properties of titanium-based alloys," in *Elsevier eBooks*, 2010, pp. 58–80, doi.org/10.1533/9781845699451.1.58.
- [2] Z. Doni, M. Buciumeanu, and L. Palaghianq, "Topographic, Electrochemical Ti6Al4V Alloy Surface Characterization in Dry and Wet Reciprocating Sliding," *Tribology in Industry*, vol. 35, no. 3, pp. 217–224, Sep. 2013.
- [3] F. Zivic, M. Babic, S. Mitrovic, and P. Todorovic, "Interpretation of the Friction Coefficient During Reciprocating Sliding of Ti6Al4V Alloy Against Al2O3," *Tribology in Industry*, vol. 33, no. 1, pp. 36–42, 2011.
- [4] H. Garbacz, P. Wicinski, M. Ossowski, G. Ortore, T. Wierzcho'na, and K.J. Kurzydłowski, "Surface engineering techniques used for improving the mechanical and tribological properties of the Ti6Al4V alloy," *Surface & Coating Technology*, vol. 202, pp. 2453–2457, Feb. 2008, doi.org/10.1016/j.surfcoat.2007.08.068.
- [5] M. Labudovic, D. Blecic, and Z. Blecic, "Decreasing of Friction and Wear of Ti-6Al-4V Alloy by Surface Modification Technique," *Tribology in Industry*, vol. 19, no. 4, pp. 146–151, 1997.
- [6] T. Tabrizi, H. Aghajani, and P. Mirzapour, "Estimation of the effect of process parameters of plasma nitriding on the surface hardness and corrosion behaviour of pure titanium by artificial neuron network," *Journal of the Balkan Tribological Association*, vol. 28, issue 5, pp. 597–612, 2022.
- [7] S.H. Dina, M.A. Shah, and N.A. Sheikh, "Effect of CVD-Diamond on the Tribological and Mechanical Performance of Titanium Alloy (Ti6Al4V)," *Tribology in Industry*, vol. 38, no. 4, pp. 530–542, Dec. 2016.
- [8] S. M. Lavrys, I. M. Pohrelyuk, O. B. Tkachuk, J. Padgurskas, V. S. Trush, and R. V. Proskurnyak, "Comparison of Friction Behaviour of Titanium Grade 2 after Non-Contact Boriding in Oxygen-Containing Medium with Gas Nitriding," *Coatings*, vol. 13, no. 2, 282, Jan. 2023, doi.org/10.3390/coatings13020282.
- [9] J.L Reynold, R.L Holdren, and L.E Brown, "Electro-Spark Deposition," *Advanced Materials Processes*, vol. 161, pp. 35–37, 2003.
- [10] Z. Zhengchuan, L. Guanjun, Ie. Konoplianchenko, V. B. Tarel'nyk, G. Zhiqin, and D. Xin, "A review of the electro-spark deposition technology," *Bulletin of Sumy National Agrarian University. The series: Mechanization and Automation of Production Processes*, vol. 44, no. 2, pp. 45–53, May 2021, doi.org/10.32845/msnau.2021.2.10.

- [11] P. J. Liew, C. Y. Yap, J. Wang, T. Zhou, and J. Yan, "Surface modification and functionalization by electrical discharge coating: a comprehensive review," *International Journal of Extreme Manufacturing*, vol. 2, no. 1, p. 012004, Feb. 2020, doi.org/10.1088/2631-7990/ab7332.
- [12] L. Chen, W. Gao, Z. Li, H. Zhang, and Z. Hu, "Electro-spark deposition of Fe-based amorphous alloy coatings," *Materials Letters*, vol. 61, no. 1, pp. 165–167, Jan. 2007, doi.org/10.1016/j.matlet.2006.04.042.
- [13] V.V. Mikhailov, E.A. Pasinkovsky, K.A. Bachu and P.V. Peretyatku, "On the issue of electrospark alloying of titanium and its alloys," *Surface engineering and applied electrochemistry*, vol. 42, issue 3, pp. 106-111, 2006.
- [14] V.V. Mikhailov, A.E. Gitlevich, A.D. Verkhoturov, A.I. Mikhaylyuk, A.V. Belyakovsky, and L.A. Konevtsov, "Electrospark alloying of titanium and its alloys, physical and technological aspects and the possibility of practical use. Short review," *Surface engineering and applied electrochemistry*, vol. 49, no 5, pp. 21–44, 2013.
- [15] A.E. Kudryashov, Z.V. Ereemeeva, E.A. Levashov, V. Yu. Lopatin, A.V. Sevostyanova, and E.I. Zamulaeva, "On Application of Carbon-Containing Electrode Materials in Technology of Electrospark Alloying: Part 1. Peculiarities of Coating Formation Using Electrospark Treatment of Titanium Alloy OT4-1," *Surface Engineering and Applied Electrochemistry*, vol. 54, no. 5, pp. 437–445, 2018, doi.org/10.3103/S1068375518050083.
- [16] T. Penyashki, G. Kostadinov, M. Kandeve, and D. Radev, "Electrospark and gas flame layering. Possibilities and Application," *Roll Company Publishing House*, 2020.
- [17] T. Penyashki et al., "Improving Surface Properties of Titanium Alloys by Electrospark Deposition with Low Pulse Energy," *Surface Engineering and Applied Electrochemistry*, vol. 58, no. 6, pp. 580–593, Dec. 2022, doi.org/10.3103/s1068375522060126.
- [18] E.A. Levashov, "Advanced Materials and Technologies of Self-Propagating High-Temperature Synthesis," *Moscow: MISIS*, 2011.
- [19] E. A. Levashov et al., "Nanoparticle dispersion-strengthened coatings and electrode materials for electrospark deposition," *Thin Solid Films*, vol. 515, no. 3, pp. 1161–1165, Nov. 2006, doi.org/10.1016/j.tsf.2006.07.140.
- [20] A. V. Kolomeichenko, I. S. Kuznetsov, A. Y. Izmaylov, R. Y. Solovyev, and S. N. Sharifullin, "Investigation of Finemet nanocrystalline alloy coating obtained by the electric spark method," *International Journal of Nanotechnology*, vol. 15, no. 4/5, p. 380, Jan. 2018, doi.org/10.1504/ijnt.2018.094794.
- [21] I.S. Kuznetsov, "Electrospark coatings of amorphous and nanocrystalline iron-based alloys," *Powder Metallurgy and Functional Coatings*, vol. 2, pp. 63-70, Jan. 2016, doi.org/10.17073/1997-308X-2016-2-63-70.
- [22] D.A. Khan, M. Hameedullah, "Effect of tool polarity on the machining characteristics in electric discharge machining of silver steel and statistical modeling of the process," *International Journal of Engineering Science and Technology (IJEST)*, vol. 3, no. 6, pp. 5001-50010, 2011.
- [23] B. B. Pradhan and B. Bhattacharyya, "Improvement in microhole machining accuracy by polarity changing technique for microelectrode discharge machining on Ti—6Al—4V," *Proceedings of the Institution of Mechanical Engineers, Part B: Journal of Engineering Manufacture*, vol. 222, no. 2, pp. 163–173, Feb. 2008, doi.org/10.1243/09544054jem959.
- [24] L. Slătineanu, H. P. Schulze, O. Dodun, M. Coteață, L. Gherman, and I. Grigoraș (Beșliu), "Electrode Tool Wear at Electrical Discharge Machining," *Key Engineering Materials.*, vol. 504-506, pp. 1189–1194, Feb. 2012, doi.org/10.4028/www.scientific.net/kem.504-506.1189.
- [25] L. Straka and S. Hašová, "Study of Tool Electrode Wear in EDM Process," *Key Engineering Materials*, vol. 669, pp. 302–310, Oct. 2015, doi.org/10.4028/www.scientific.net/kem.669.302.
- [26] P. M. Brochu, M. J. Milligan, M. D. W. Heard, and M. S. Cadney, "Bulk Nanostructure and Amorphous Metallic Components Using the Electrospark Welding Process," *Assembly Automation*, vol. 30, no. 3, Jan. 2010, doi.org/10.1108/14451541080001491.
- [27] S. Cadney, G. Goodall, G. Kim, A. Moran, and M. Brochu, "The transformation of an Al-based crystalline electrode material to an amorphous deposit via the electrospark welding process," *Journal of Alloys and Compounds*, vol. 476, no. 1-2, pp. 147–151, May 2009, doi.org/10.1016/j.jallcom.2008.09.017.
- [28] V. Mihailov et al., "Synthesis of Multicomponent Coatings by Electrospark Alloying with Powder Materials," *Coatings*, vol. 13, no. 3, p. 651, Mar. 2023, doi.org/10.3390/coatings13030651.
- [29] E.A. Levashov, O.Y. Malochkin, A.E. Kudryashov, et al., "Influence of nano-sized powders on combustion processes and formation of composition, structure, and properties of alloys of the system Ti-Al-B," *Journal of Non-Ferrous Metals*, no. 1, pp. 54-59, 2003.

- [30] E.A. Levashov, A.E. Kudryashov, Yu.S. Pogozhev, et al., "An investigation of the influence of the parameters of pulse discharges on mass transfer, structure, composition, and properties of TiC-NiAl-based electrical spark coatings modified by nanodispersed components," *Journal of Non-Ferrous Metals*, vol. 45, no. 11, pp. 32-40, 2004.
- [31] T. Penyashki, G. Kostadinov, M. Kandeve, V. Kamburov, A. Nikolov, and R. Dimitrova, "Abrasive and Erosive Wear of Ti6Al4V Alloy with Electrospark Deposited Coatings of Multicomponent Hard Alloys Materials Based of WC and TiB₂," *Coatings*, vol. 13, no. 1, p. 215, Jan. 2023, doi.org/10.3390/coatings13010215.
- [32] M. Kandeve, T. Penyashki, G. Kostadinov, and Z. Kalichin, "Abrasive and Erosion Wear of Composite NiCrSiB Coatings Inflicted with Subsonic Flammable Structure through a Cold Process," *IOP Conference Series*, vol. 724, p. 012014, Jan. 2020, doi.org/10.1088/1757-899x/724/1/012014.
- [33] M. Kandeve, G. Kostadinov, T. Penyashki, V. Kamburov, R. Dimitrova, S. Valcanov, A. Nikolov, B. Elenov, and M. Petrzhik, "Abrasive Wear Resistance of Electrospark Coatings on Titanium Alloys," *Tribology in Industry*, vol. 44, no. 1, pp. 132-142, Mar. 2022, doi.org/10.24874/ti.1143.06.21.09.
- [34] Trotsky, S. Petrovich, V. Andreeva, A. Popovich, and M. Zamozdra, "Synthesis Of Ceramics Titanium Compounds By Mechanical Alloying Of Tib₂-Tin Systems," *Metal*, May 2021, doi.org/10.37904/metal.2021.4204.
- [35] P. V. Kiryukhantsev-Korneev, D. V. Shtansky, M. I. Petrzhik, E. A. Levashov, and B. N. Mavrin, "Thermal stability and oxidation resistance of Ti-B-N, Ti-Cr-B-N, Ti-Si-B-N and Ti-Al-Si-B-N films," *Surface & Coatings Technology*, vol. 201, no. 13, pp. 6143-6147, Mar. 2007, doi.org/10.1016/j.surfcoat.2006.08.133.
- [36] J. Padgurskas et al., "Tribological properties of coatings obtained by electro-spark alloying C45 steel surfaces," *Surface & Coatings Technology*, vol. 311, pp. 90-97, Feb. 2017, doi.org/10.1016/j.surfcoat.2016.12.098.
- [37] S. A. Pyachin, A. A. Burkov, and V. S. Komarova, "Formation and study of electrospark coatings based on titanium aluminides," *Journal of Surface Investigation: X-ray, Synchrotron and Neutron Techniques*, vol. 7, no. 3, pp. 515-522, May 2013, doi.org/10.1134/s1027451013030336.
- [38] C. Benoualia, M.N. Bachirbeya, and T. Sayaha, "Effect of the Normal Load on the Friction and Wear Behaviour of Nickel-based Alloys Ni-Cr-B-Si-C-W," *Tribology in Industry*, vol. 42, no. 4, pp. 547-555, Dec. 2020, doi.org/10.24874/ti.832.01.20.09.
- [39] A. Vencl, M. Mrdak, and P. Hvizdos, "Tribological Properties of WC-Co/NiCrBSi and Mo/NiCrBSi Plasma Spray Coatings under Boundary Lubrication Conditions," *Tribology in Industry*, vol. 39, no. 2, pp. 183-191, Jun. 2017, doi.org/10.24874/ti.2017.39.02.04.
- [40] G. Khosravi, M.H. Sohi, H. Ghasemi, and N.J. Karazmoudeh, "Study of the Tribological Properties of Diffusion Coated NiTi Intermetallic on Cp Titanium," *Tribology in Industry*, vol. 44, no. 4, pp. 632-640, Dec. 2022, doi.org/10.24874/ti.1326.07.22.09.